Chemical Geology 382 (2014) 24–31

Contents lists available at ScienceDirect

Chemical Geology

journal homepage: www.elsevier.com/locate/chemgeo

# Methane sources and sinks in the subtropical South Pacific along 17°S as traced by stable isotope ratios

Chisato Yoshikawa [a,*], Elena Hayashi [a], Keita Yamada [a], Osamu Yoshida [b], Sakae Toyoda [a], Naohiro Yoshida [a,c]

[a] Interdisciplinary Graduate School of Science and Engineering, Tokyo Institute of Technology, 4259 Nagatsuta-cho, Midori-ku, Yokohama- city, 226-8503, Japan
[b] Department of Environmental and Symbiotic Science, College of Agriculture, Food and Environment Sciences, Rakuno Gakuen University, 582 Bunkyodai-Midorimachi, Ebetsu, Hokkaido, 069-8501, Japan
[c] Earth-Life Science Institute, Tokyo Institute of Technology, 2-12-1 Ookayama, Meguro-ku, Tokyo, 152-8551, Japan

ARTICLE INFO

*Article history:*
Received 4 April 2013
Received in revised form 14 May 2014
Accepted 15 May 2014
Available online 2 June 2014

Editor: Michael E. Böttcher

*Keywords:*
Stable isotopes
Methane sources and sinks
Marine methane flux
Subtropical South Pacific

ABSTRACT

We analyzed the concentration and stable carbon isotopic ratio ($\delta^{13}C$-$CH_4$) of methane in the atmosphere and in dissolved methane in water column along 17°S in the subtropical South Pacific. Additionally, the hydrogen isotopic ratios ($\delta D$-$CH_4$) of some water samples were analyzed. The sea–air $CH_4$ flux is high in the eastern region and off the west coast of Australia, which is related to the high concentrations of dissolved $CH_4$ and high wind speeds. Moreover, there is a positive correlation between the $CH_4$ and chlorophyll *a* concentrations at the surface. This consistency suggested that active $CH_4$ productions related to the primary production cause surface $CH_4$ accumulation. $CH_4$ shows a decrease in concentration and an increase in $\delta^{13}C$-$CH_4$ and $\delta D$-$CH_4$ values from the surface to the depth of about 1000 m. The relationship between $\delta^{13}C$-$CH_4$ values and $CH_4$ concentration indicates that the isotopic enrichment of $CH_4$ reflects microbial oxidation of $CH_4$ with isotopic fractionation during vertical transport via vertical sinking and/or zooplankton migration. East of 120°W, $\delta^{13}C$-$CH_4$ values at around 1000 m exceed −30.0‰. The relationships among the $\delta^{13}C$-$CH_4$ values, $CH_4$ concentrations, and oxygen concentrations indicate that the $^{13}C$-enriched $CH_4$ originates not only from in situ $CH_4$ production and oxidation but also from $CH_4$ transported from the eastern margin off Peru. Furthermore, at a site near the Central Lau Spreading Centers in the Lau Basin, high $\delta^{13}C$-$CH_4$ values (up to −21.4‰) are observed in the benthic water, suggesting a hydrothermal field source.



## 1. Introduction

Methane ($CH_4$) is the second most important anthropogenic greenhouse gas after carbon dioxide (IPCC, 2007). Although major sources and sinks of atmospheric $CH_4$ have been identified, great uncertainties remain in the estimation of the sources, sinks, and atmospheric budget of $CH_4$. Estimates of the $CH_4$ flux from the ocean vary from 4 to 15 Tg $yr^{-1}$ (Houweling et al., 2000; Wuebbles and Hayhoe, 2002). In general, the $CH_4$ concentration in the oceans gradually decreases with increasing depth, a phenomenon that is controlled by $CH_4$ inputs from methanogenesis and removal by oxidation (e.g., Scranton and Brewer, 1977; Coleman et al., 1981). The repeated observation of supersaturation in surface water is known as the "ocean methane paradox." Previous studies have suggested that the source of this excess methane is methanogenic archaea living within anaerobic cavities of the zooplankton gut and anaerobic environments inside sinking particles (e.g., Karl and Tilbrook, 1994; Reeburgh, 2007; Pack et al., 2011; Valentine, 2011). Recently, Karl et al. (2008) and Metcalf et al. (2012) suggested that $CH_4$ is produced by aerobic bacteria as a byproduct of methylphosphonate decomposition in phosphate-stressed surface waters, and Damm et al. (2010) suggested that $CH_4$ production related to dimethylsulfoniopropionate occurs even in phosphate-rich surface waters. Furthermore, diagenesis of sedimentary organic matter, abiotic production in hydrothermal systems, and decomposition of $CH_4$ clathrate hydrates are source processes emitting $CH_4$ from the seafloor to the water column (e.g., Reeburgh, 2007).

Stable carbon and hydrogen isotope ratios of dissolved $CH_4$ ($\delta^{13}C$-$CH_4$ and $\delta D$-$CH_4$) provide information about $CH_4$ sources and sinks. The $\delta^{13}C$-$CH_4$ value of the surface of the open ocean is similar to the atmospheric equilibrium value of about −47‰ (Grant and Whiticar, 2002). Previous studies have observed isotopically enriched $\delta^{13}C$-$CH_4$ values at the depth of maximum $CH_4$ concentration above the pycnocline (e.g., Holmes et al., 2000; Sasakawa et al., 2008). Sasakawa et al. (2008) observed that the $\delta^{13}C$ of $CH_4$ produced from zooplankton ranges from −54 to −61‰ and that the $\delta^{13}C$ of $CH_4$ produced from sinking particles ranges from −37 to +6‰. The sources of this $CH_4$ are methanogenic archaea living within anaerobic cavities of the zooplankton gut and

* Corresponding author at: Department of Biogeochemistry, Japan Agency for Marine–Earth Science and Technology, 2-15 Natsushima-cho, Yokosuka city, 237-0061, Japan. Tel.: +81 46 867 9786.
*E-mail address:* yoshikawac@jamstec.go.jp (C. Yoshikawa).

http://dx.doi.org/10.1016/j.chemgeo.2014.05.024

anaerobic environments inside sinking particles, followed by oxidation prior to release. From these results, they suggested that the supersaturated $CH_4$ in the surface mixed layer in the northwestern North Pacific is produced mainly from sinking particles. Moreover, a culture study by Coleman et al. (1981) revealed that carbon isotopic fractionation during microbial oxidation of $CH_4$ ranges from 1.013 to 1.025 and that the hydrogen isotopic fractionation ranges from 1.103 to 1.325. The degree of progress of $CH_4$ oxidation or initial concentration before $CH_4$ oxidation can be estimated from observed $\delta^{13}$C-$CH_4$ and $\delta$D-$CH_4$ values with these fractionation factors. Furthermore, the $CH_4$ emitted from biogenic sources such as sedimentary organic matter and $CH_4$ clathrate hydrates has isotopically depleted values ($\delta^{13}C = -56$ to $-73$‰: Kvenvolden, 1993; $\delta^{13}C = -65$ to $-68$‰ and $\delta D = -197$ to $-199$‰: Kastner et al., 1998), and the $CH_4$ emitted from abiotic and thermogenic productions in hydrothermal systems has isotopically enriched values ($\delta^{13}C = -24.6$ to $-28.9$‰ and $\delta D = -122$ to $-135$‰: Botz et al., 2002; $\delta^{13}C = -20$‰: Faure et al., 2010). Thus, these benthic processes can be distinguished by measuring benthic $\delta^{13}$C-$CH_4$ and $\delta$D-$CH_4$ values (e.g., Whiticar, 1999). In this study, $CH_4$ concentrations and $\delta^{13}$C-$CH_4$ and $\delta$D-$CH_4$ values were measured to reveal the sources and sinks of $CH_4$ in the subtropical South Pacific.

## 2. Materials and methods

Water and air sampling and conductivity, temperature, and depth (CTD) observations were conducted along 17°S in the subtropical South Pacific during cruise MR09-01 of the R/V Mirai, Japan Agency for Marine–Earth Science and Technology (JAMSTEC), in April–June 2009 (Fig. 1a). Water samples for the measurement of $CH_4$ concentration and $\delta^{13}$C-$CH_4$ analysis were collected from 13 profiles (St. X19, 66, 85, 104, 121, 134, 152, 174, 189, 209, 229, 255, and 285) and water samples for $\delta$D-$CH_4$ analysis were collected from 3 profiles (St. 66, 121, and 174) with rosette-mounted Niskin bottles. The samples were then transferred to 125-mL glass vials for $\delta^{13}$C-$CH_4$ analysis and 600-mL glass vials for $\delta$D-$CH_4$ analysis. After an approximately two-fold volume overflow, 20 μL for the 125-mL vials and 100 μL for the 600-mL vials of saturated $HgCl_2$ solution were added, so that the final concentrations of $HgCl_2$ in the samples were 10 mg $L^{-1}$. The vials were sealed with butyl rubber and aluminum caps and stored in dark conditions at 4 °C until analysis. Air samples for $\delta^{13}$C-$CH_4$ analysis were collected in pre-vacuumed 200-mL glass bulbs from 10 m above the sea surface at the same locations as the water sampling stations. The data and analytical procedures for water temperature, salinity, oxygen, and chlorophyll *a* concentrations are available in the Data Research System for Whole Cruise Information at JAMSTEC (http://www.godac.jamstec.go.jp/cruisedata/mirai/e/index.html).

The $\delta^{13}$C values and concentrations of $CH_4$ were determined by gas chromatography/combustion/isotope ratio mass spectrometry (GC-C-IRMS) at the Tokyo Institute of Technology using the method of Tsunogai et al. (1998, 2000). The $\delta$D values of $CH_4$ were determined by gas chromatography/high-temperature conversion/isotope ratio mass spectrometry (GC-TC-IRMS) at the Tokyo Institute of Technology using the method of Yamada et al. (2003). The data are reported in delta notation as follows: $\delta^{13}C = (({}^{13}C/{}^{12}C)_{sample}/({}^{13}C/{}^{12}C)_{VPDB} - 1) \times 1000$ and $\delta D = (({}^{2}H/{}^{1}H)_{sample}/({}^{2}H/{}^{1}H)_{VSMOW} - 1) \times 1000$. The precision of these analyses was 6.5% for the concentrations, ±0.2‰ for $\delta^{13}$C, and ±3‰ for $\delta$D.

The saturation ratio (SR) of dissolved $CH_4$ was calculated from the observed concentration of dissolved $CH_4$ ($C_w$) and the concentration

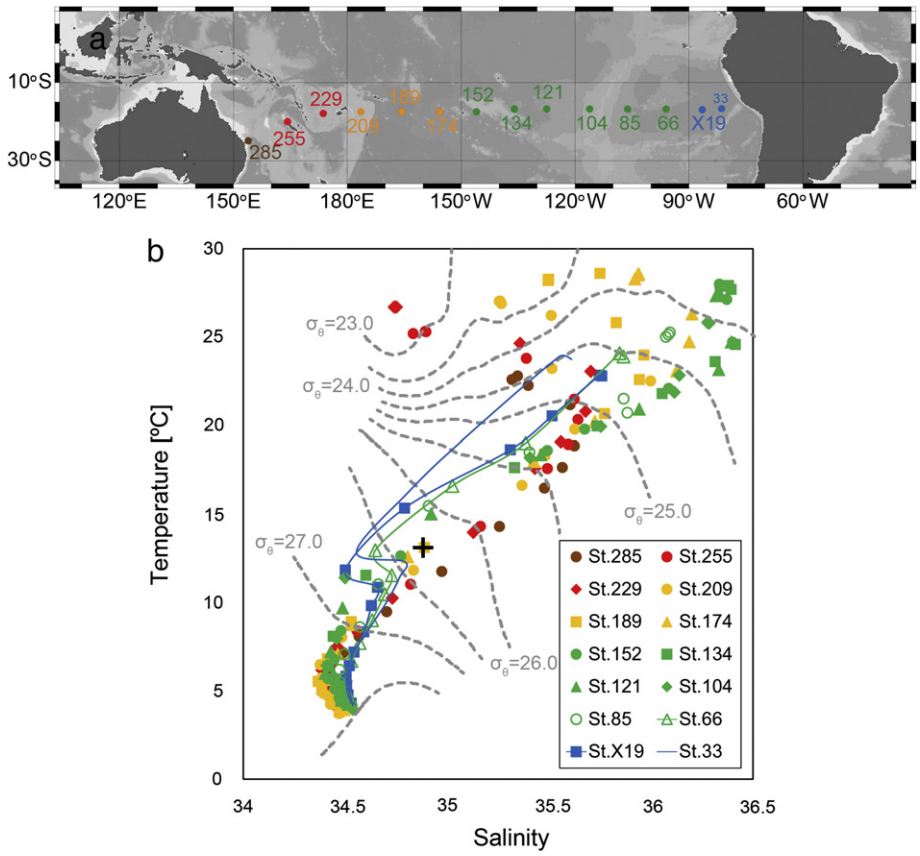


**Fig. 1.** Map of the subtropical South Pacific showing the locations of the hydrocast stations (a) and a T–S diagram (b) for the MR09-01 cruise. The plots are color-coded according to area (blue: HUMB, green: E-SPSG, orange: C-SPSG, red: ARCH, and brown: AUSE). The line with no symbol indicates the easternmost station without isotopic analyses from the MR09-01 cruise. A black cross indicates ESSW.

of $CH_4$ in water equilibrated with ambient air ($C_a$), which was calculated using the solubility equation of Wiesenburg and Guinasso (1979):

$$SR(\%) = (C_w/C_a - 1) \times 100. \quad (1)$$

The sea–air $CH_4$ flux (F) was calculated from

$$F\left(\mu mol\ m^{-2}\ day^{-1}\right) = k_w \times \left(C_{w\ (0-50\ m)} - C_a\right). \quad (2)$$

$k_w$ is the gas transfer coefficient conventionally expressed as a function of wind speed:

$$k_w = 0.39\nu^2 (S_c/660)^{-0.5}, \quad (3)$$

where $S_c$ is the Schmidt number for $CH_4$ in seawater (Wanninkhof, 1992). The wind speeds used in this work ($\nu$) were the monthly means for July 2009 at each station, obtained from the National Centers for Environmental Prediction (NCEP) website (http://www.esrl.noaa.gov/psd/data/gridded/data.ncep.reanalysis.derived.surface.html).

## 3. Results and discussion

### 3.1. Oceanographic setting

The stations were categorized into five area types according to Longhurst (2006) (Fig. 1a). From the east, these include the Humboldt Current Coastal Province (HUMB), containing the coastal boundary current system off the west coast of South America; the Eastern South Pacific Subtropical Gyre Province (E-SPSG), which is the northeastern part of the subtropical gyre of the South Pacific Ocean; the Central South Pacific Subtropical Gyre Province (C-SPSG), which is the northern central part of the subtropical gyre of the South Pacific Ocean; the Archipelago Deep Basins Province (ARCH), an area containing many islands; and the East Australian Coastal Province (AUSE), including the East Australian Current.

Fig. 1b shows a T–S diagram color-coded according to area. In the HUMB, Equatorial Subsurface Water (ESSW), which has a density near 26.5 $\sigma_\theta$ and is typically salty, oxygen-poor, and nutrient-rich (black cross in Fig. 1b) (De Pol-Holz et al., 2009), is entrained at a depth of around 250 m from the eastern margin off Peru and transported westward along the South Equatorial Current. In the E-SPSG, the features of the ESSW gradually fade toward the center, and sea surface salinity in our study area increases to a maximum value of 36.4. Sea surface salinity decreases again west of the C-SPSG, reaching a minimum value of 34.7 in the ARCH because of heavy rainfall related to the Intertropical Convergence Zone (ITCZ). In the AUSE, the East Australian Current flows southward at the surface along the east coast of Australia, creating a water mass structure that differs from that in the ARCH.

### 3.2. Sea–air $CH_4$ flux

The fluxes of $CH_4$ from the surface ocean to the atmosphere in the subtropical South Pacific were calculated using Eqs. (1)–(3) with the observed mean atmospheric $CH_4$ concentration (1.70 ppmv) and were found to range from −0.2 to +4.8 μmol $m^{-2}$ $day^{-1}$ (Table 1). The flux has high values at the eastern sites of stations X19, 66, and 85 (+1.4 to +4.8 μmol $m^{-2}$ $day^{-1}$) and at the western coastal sites of stations 255 and 285 (+1.3 to +2.4 μmol $m^{-2}$ $day^{-1}$), but low values in the C-SPSG (St. 174, 189, and 209). The high fluxes at the eastern sites and the western coastal sites reflect the dominating effects of high concentrations of dissolved $CH_4$, exceeding 2 nmol $kg^{-1}$, and high wind speeds, exceeding 8 m $s^{-1}$.

The $\delta^{13}$C-$CH_4$ values of ambient air range from −47.0 to −46.4‰ with an average value of −46.7‰ (Table 1). The mean dissolved $\delta^{13}$C-$CH_4$ values in the mixed layer (0–50 m) range from −53.2 to −45.7‰, much larger spatial variation than what was seen in the atmospheric values. The larger variability in water than in air seems to be due to faster mixing in the air than in the water. Sansone et al. (2001) suggested that upwelling induced anoxic regions are major sites of $CH_4$ accumulation and provide significant atmospheric inputs of isotopically heavy $CH_4$. The maximum sea–air flux of +4.8 μmol $m^{-2}$ $day^{-1}$ and the highest $\delta^{13}$C-$CH_4$ values of −45.7‰ occur at station 66, where the oxygen-poor ESSW is entrained to the subsurface layer and the oxygen concentration has the minimum value of 4 μmol $kg^{-1}$ in our study area (see Figs. 1b and 2d).

### 3.3. Surface and subsurface $CH_4$ and $\delta^{13}$C-$CH_4$ distribution

$CH_4$ concentrations above 400 m water depth range from 0.9 to 2.7 nmol $kg^{-1}$ (Fig. 2b). Except for sites in the C-SPSG (St. 209, 189, and 174) and at some depths at stations 104 and 85, $CH_4$ is supersaturated above a depth of 100 m (up to 46.9%) (Fig. 3a), as observed in previous studies (e.g., Conrad and Seiler, 1988; Tilbrook and Karl, 1995; Sasakawa et al., 2008). This suggests formation of $CH_4$ in the surface water. Because phytoplankton do not generate $CH_4$ directly, the supersaturating $CH_4$ must result from microbial methanogenesis during zooplankton grazing and particle sinking (e.g., Karl and Tilbrook, 1994; Reeburgh, 2007). The $CH_4$ concentration in the euphotic layer above 200 m generally decreases from the eastern region (HUMB) to the western region (ARCH) and increases in western coastal sites

**Table 1**
Wind speeds, surface ocean $CH_4$ concentrations, sea–air $CH_4$ fluxes, and atmospheric and surface ocean isotopic ratios.

| Station number | Latitude | Longitude | Wind speed ($ms^{-1}$) | Dissolved $CH_4$ conc. $_{ave.\ 0-50\ m}$ (nmol $kg^{-1}$) | Sea–air flux (μ mol $m^{-2}$ $day^{-1}$) | $\delta^{13}$C-$CH_{4\ air}$ (‰) | $\delta^{13}$C-$CH_{4\ ave.\ 0-50\ m}$ (‰) |
|---|---|---|---|---|---|---|---|
| X19 | 16.8°S | 86.4°W | 9.2 | 2.10 | 1.4 | −46.5 | −46.9 |
| 66 | 16.8°S | 96.0°W | 9.5 | 2.40 | 4.8 | −46.7 | −45.7 |
| 85 | 16.8°S | 106.0°W | 8.9 | 2.00 | 1.5 | −46.8 | −46.4 |
| 104 | 16.8°S | 116.0°W | 8.7 | 1.90 | 0.9 | −47.0 | −47.3 |
| 121 | 16.8°S | 127.3°W | 7.7 | 2.02 | 1.8 | −46.7 | −* |
| 134 | 16.8°S | 136.0°W | 7.0 | 1.80 | 0.4 | −46.5 | −46.2 |
| 152 | 17.5°S | 145.8°W | 7.0 | 2.05 | 1.8 | −46.6 | −* |
| 174 | 17.5°S | 155.7°W | 7.9 | 1.67 | −0.2 | −46.7 | −** |
| 189 | 17.5°S | 165.7°W | 7.8 | 1.78 | 0.5 | −46.7 | −53.2 |
| 209 | 17.5°S | 176.3°W | 6.2 | 1.96 | 0.8 | −46.4 | −46.6 |
| 229 | 17.8°S | 173.7°E | 7.4 | 1.81 | 0.2 | −46.6 | −45.7 |
| 255 | 20.0°S | 164.4°E | 8.3 | 2.13 | 2.4 | −46.6 | −45.9 |
| 285 | 24.9°S | 154.1°E | 8.3 | 2.12 | 1.3 | −46.6 | −47.1 |

* There is no 50 m data.
** There is no 0 m data.

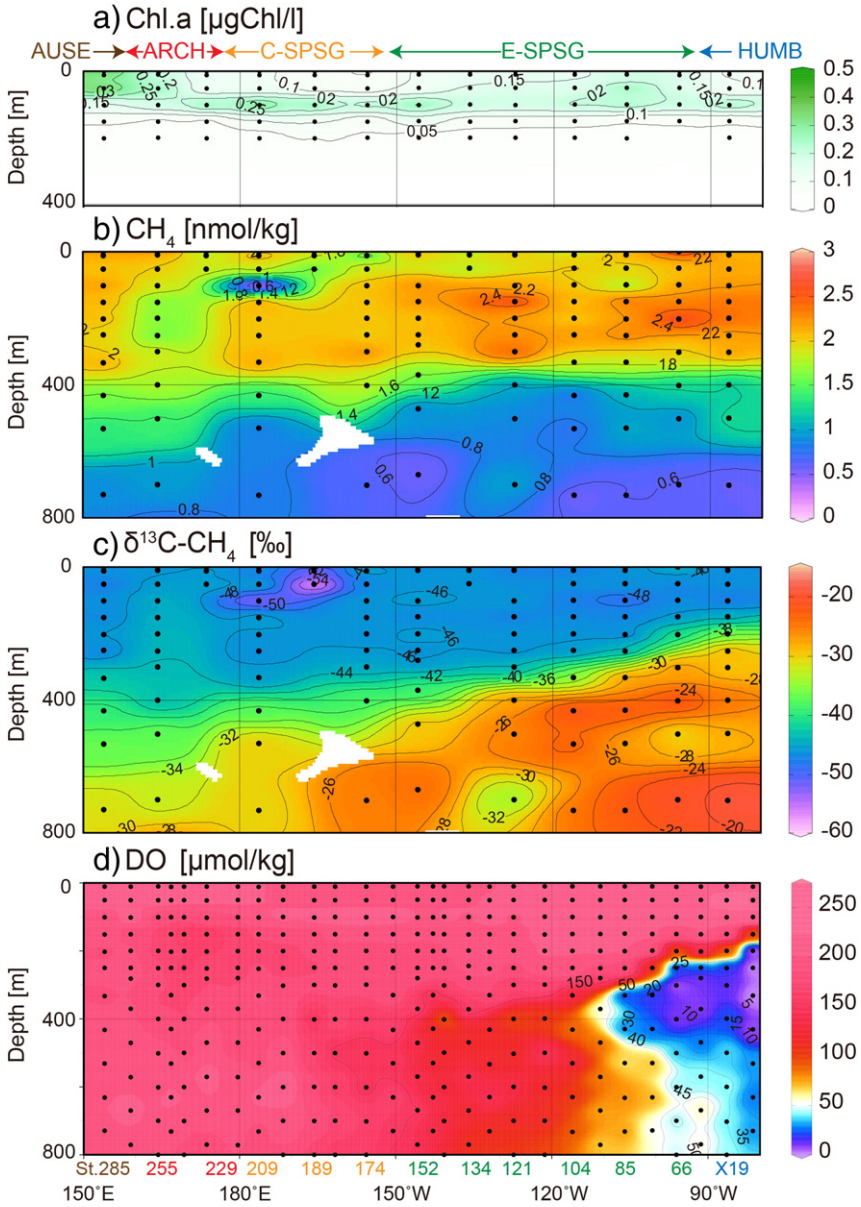


**Fig. 2.** Horizontal distributions of chlorophyll *a* concentration (a), $CH_4$ concentration (b), $\delta^{13}C$-$CH_4$ values (c) and dissolved oxygen concentration (d) above 800 m along 17°S. The black dots indicate sampling points.

(AUSE) (Fig. 2b). The chlorophyll *a* concentration generally decreases from east to west, increases at the surface in the coastal stations, and shows high values in the subsurface water at approximately 100 m in the C-SPSG (Fig. 2a). There is a positive correlation between chlorophyll *a* and $CH_4$ concentrations at the surface (Fig. 3d), but there is an inverse correlation in the subsurface water in the C-SPSG (Fig. 2a and b). The inconsistency in the subsurface water in the C-SPSG is discussed later in this section.

Except for sites in the C-SPSG (St. 209 and 189) and at some depths of stations 104, 85, and X19, $^{13}C$ enrichment relative to the atmospheric value of −47‰ occurred in the water from the surface to 800 m (Fig. 2c), as observed in previous studies (e.g., Holmes et al., 2000; Sansone et al., 2001; Sasakawa et al., 2008). The recent isotopic results of Sasakawa et al. (2008) suggest that the isotopically enriched $CH_4$, which ranges from −36.7 to +5.9‰, is emitted from sinking particles through microbial methanogenesis and microbial $CH_4$ oxidation within the oxic/anoxic boundary of the particles, even in the surface water above a depth of 100 m. As it is related to primary production, the $CH_4$ production within anaerobic environments inside sinking particles causes $CH_4$ accumulation in the water from the surface to 800-m depths. The $\delta^{13}C$-$CH_4$ values in the water between depths of 400 and 800 m decrease from east to west (Figs. 2c and 3b). The $^{13}C$-enriched $CH_4$ below the depth of 400 m in the eastern region is discussed later in the next section.

In the C-SPSG and at some depths of stations 104, 85, and X19, $CH_4$ has isotopically depleted values (min: −57.5‰), which are much less than the atmospheric value of −47‰, and relatively low concentrations compared to the surrounding surface water (Fig. 2). Especially at stations 209 and 85, the observed depths of isotopically depleted values and low concentrations of $CH_4$ are consistent with chlorophyll *a* maximum depths (Fig. 3). Sasakawa et al. (2008) revealed that the $CH_4$ emitted from zooplankton has much lower $\delta^{13}C$-$CH_4$ values, which range from −61.3 to −54.4‰, than that from sinking particles (−36.7 to +5.9‰) or the atmosphere (−47‰). The $CH_4$ in the euphotic layer in the C-SPSG may be affected by $CH_4$ emission from zooplankton guts. Alternatively, Karl et al. (2008) suggested that $CH_4$ is produced by aerobic bacteria as a

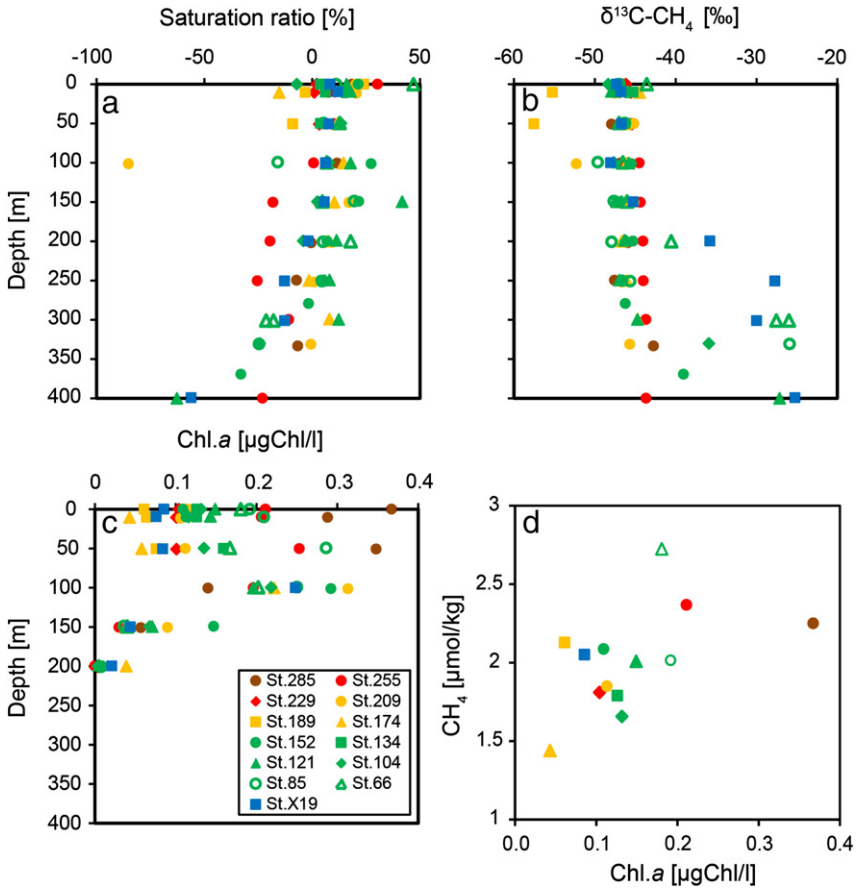


**Fig. 3.** Vertical distributions of the dissolved $CH_4$ saturation ratio (a), $\delta^{13}C$-$CH_4$ values (b) and chlorophyll *a* concentrations (c) above 400-m depths and the relationship between chlorophyll *a* and $CH_4$ concentration in the surface water (d).

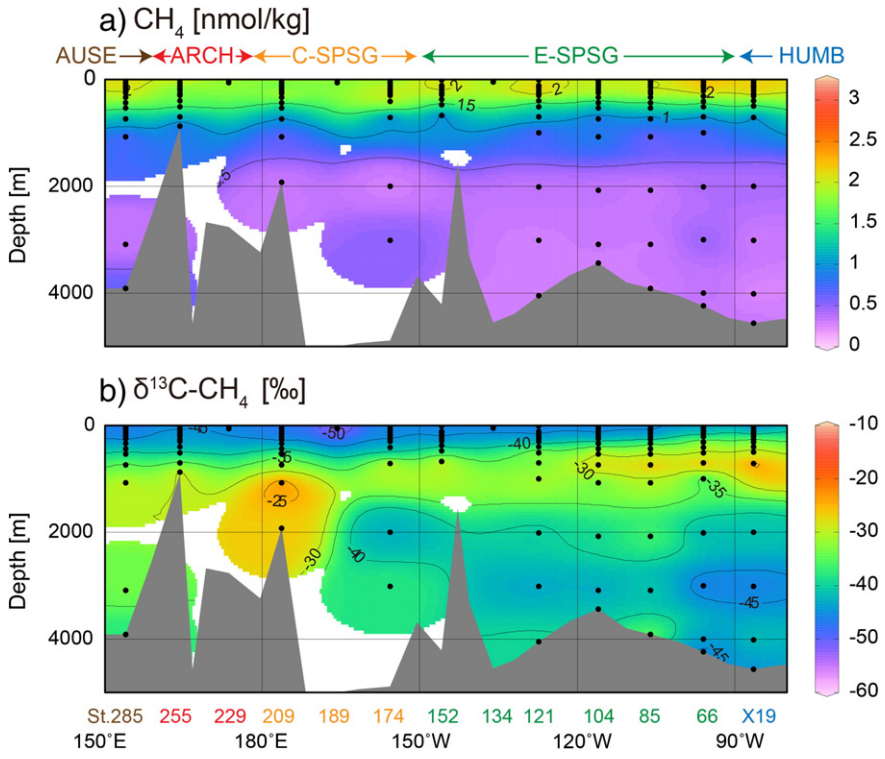


**Fig. 4.** Horizontal distributions of $CH_4$ concentrations (a) and $\delta^{13}C$-$CH_4$ values (b) along 17°S. The black dots indicate sampling points.

byproduct of methylphosphonate decomposition in phosphate-stressed waters. Because a phosphorus deficit compared to nitrogen was observed in the C-SPSG during our cruise, the $CH_4$ in the euphotic layer in the C-SPSG may also be affected by aerobic $CH_4$ production.

### 3.4. Deep water $CH_4$ and $\delta^{13}C$-$CH_4$ distribution

$CH_4$ is accumulated above 1000 m; the concentrations below the depth of 1000 m are less than 1 nmol $kg^{-1}$ in our entire study area (Fig. 4a). The $\delta^{13}C$-$CH_4$ values are close to −47‰ at the surface and increase with depth above 1000 m, as observed in previous studies (e.g., Sansone et al., 2001) (Fig. 4b). The isotopically heavy $CH_4$ of low concentration reflects microbial oxidation of $CH_4$ with isotopic fractionation during vertical transport by particle sinking and/or zooplankton migration (Coleman et al., 1981).

The maximum values of $\delta^{13}C$-$CH_4$ exceed −30.0‰ east of 120°W and reach −19.3‰ at station X19. The water of the $\delta^{13}C$-$CH_4$ maximum is oxygen-poor and nutrient-rich and advects from the eastern upwelling region off Peru, where surface primary production is very high and $CH_4$ hydrate occurs in sediment (Pecher et al., 2001). Similar entrainments of isotopically heavy $CH_4$ near $CH_4$ hydrate have been reported along the California shelf (Tilbrook and Karl, 1995; Valentine et al., 2001), the Oregon shelf (Rehder et al., 2002), and in the eastern tropical North Pacific (Sansone et al., 2001). These results suggest that the high primary production in the eastern upwelling region causes $CH_4$ accumulation in the water column and/or sediments and that the $CH_4$ is then oxidized with isotopic fractionation during horizontal advection. From these results, we speculate that the $^{13}C$-enriched $CH_4$ in the eastern region is transported with the South Equatorial Current from the eastern margin off Peru.

At station 209 (176.3°W, 17.5°S), the $\delta^{13}C$-$CH_4$ values are −21.4‰ at 1000 m and −26.6‰ at 2000 m, which indicate a significant enrichment in $^{13}C$ compared with the values of the surrounding sites (e.g., −42.7‰ at 2000 m at St. 174) (Fig. 4b). In the western South Pacific, isotopically heavy $CH_4$ originating from hydrothermal gas has been reported in the Havre Trough off the North Island of New Zealand (−24.6 to −28.9‰: Botz et al., 2002; −20‰: Faure et al., 2010). Station 209 is located near the Central Lau Spreading Centers in the Lau Basin (Martinez et al., 2006). The Lau Basin and the Havre Trough, which are back-arc basins in the southwestern Pacific, contain several seafloor spreading centers and hydrothermal fields (e.g., Botz et al., 2002; Martinez et al., 2006; Kim et al., 2009; Faure et al., 2010; Mottl et al., 2011). Although a hydrothermal plume containing high concentrations of $CH_4$ has been reported in the northeast Lau Spreading Centers (174.3°W, 16.4°S), which are within several kilometers of station 209 (Kim et al., 2009), no hydrothermal venting has been reported at station 209, and no temperature deviation was observed at this depth. From these results, we speculate that $CH_4$ hydrothermal venting occurs somewhere near station 209 and that the isotopically heavy $CH_4$ originating from abiogenic and/or thermogenic methanogenesis is then oxidized with isotopic fractionation during advection before arriving at station 209.

### 3.5. $CH_4$ production and consumption processes

$CH_4$ production and consumption processes can be identified by investigating the relationships between the $\delta^{13}C$-$CH_4$ value and the natural logarithm of the $CH_4$ concentration (ln[$CH_4$]) (Fig. 5).

The relationships between $\delta^{13}C$-$CH_4$ and the ln[$CH_4$] in most of the surface water, with the exception of the data for the suspected aerobic $CH_4$ production region in the C-SPSG, are concentrated around a single point ($\delta^{13}C$-$CH_4$ = −47‰ and ln[$CH_4$] = 0.7). The point reflects supersaturated $CH_4$ resulting from surface primary production and subsequent degradation. If microbial oxidation of the $CH_4$ proceeds slowly during the transportation of the $CH_4$ to the deeper layer by particle sinking and/or zooplankton migration, Eq. (4) can be applied with the assumption of a closed system. When microbial $CH_4$ oxidation occurs, the $\delta^{13}C$-$CH_4$ value increases according to

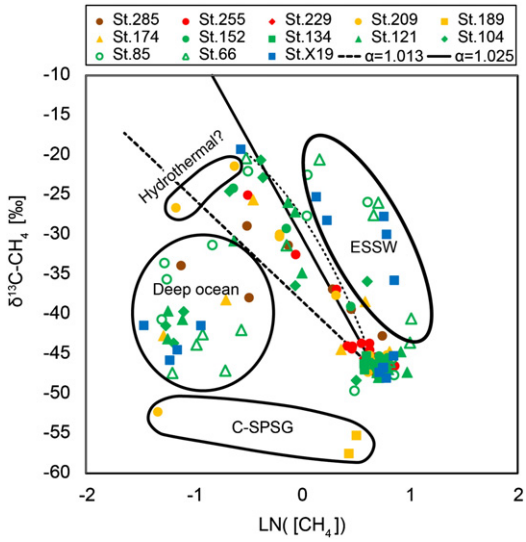


**Fig. 5.** Relationships between $\delta^{13}C$-$CH_4$ values and the natural logarithm of dissolved $CH_4$ concentrations. The solid and dashed lines indicate changes in the $\delta^{13}C$ value and $CH_4$ concentration in the case of microbial $CH_4$ oxidation with fractionation factors of 1.013 and 1.025, respectively. The dotted line indicates mixing of the most $CH_4$-enriched water with surface water.

$$\delta^{13}C{-}CH_4 = \delta^{13}C{-}CH_{4\,initial} + 1000 \times (1/\alpha{-}1) \times \ln\left([CH_4]/[CH_4]_{initial}\right), \quad (4)$$

where $\delta^{13}C$-$CH_{4\,initial}$ and $[CH_4]_{initial}$ are the $\delta^{13}C$-$CH_4$ value and concentration of $CH_4$ before the oxidation. In this case, the $CH_4$ resulting from surface primary production and subsequent degradation would establish the initial values ($\delta^{13}C$-$CH_{4\,initial}$ = −47‰ and ln[$CH_4$]$_{initial}$ = 0.7). α represents the fractionation factor during microbial oxidation, which ranges from 1.013 to 1.025 (Coleman et al., 1981). Lines indicate changes in the $\delta^{13}C$ and concentration of $CH_4$ values during partial oxidation by bacteria, the two cases of the observed lower limit (α = 1.013) and upper limit (α = 1.025), are also shown in Fig. 5. Approximately 80% of the data above 1000 m, except at the HUMB and the eastern end of the E-SPSG (see data within the circle of the ESSW in Fig. 5) and at the C-SPSG (see data within the circle of the C-SPSG in Fig. 5), plot around these two lines. These results suggest that the subsurface $CH_4$ is produced as a result of surface primary production and subsequent degradation and is subsequently affected by microbial oxidation during vertical transportation. Moreover, although we only measured δD-$CH_4$ values above 400 m depth at stations 66 and 121 and above 300 m depth at station 174, δD-$CH_4$ values range from −141 to −121‰ in the surface water above 100 m and increase with decreasing concentrations, as observed in the $\delta^{13}C$-$CH_4$ values (Fig. 6a). The δD-$CH_4$ values at 400 m are −49.7‰ at station 66 and +49.5‰ at station 121, which are within the estimated oxidized values of −67–+46‰ at station 66 and +23–+331‰ at station 121 with the observed hydrogen isotopic fractionation during microbial oxidation (α = 1.103–1.325: Coleman et al., 1981). These δD-$CH_4$ results are consistent with the previously mentioned suggestion.

At the HUMB and eastern side of the E-SPSG, the subsurface data plot above the estimated oxidation and mixing lines (Fig. 5). If the $\delta^{13}C$-$CH_4$ value originating from surface primary production and subsequent degradation is about −47‰, by using Eq. (4) and the 250 m data at station X19 ($\delta^{13}C$-$CH_4$ = −27.7‰ and [$CH_4$] = 2.14 nmol$kg^{-1}$), which are the farthest data from the lines, we estimate that 20% and 43% of the subsurface $CH_4$ originated from in situ surface primary production and subsequent degradation of detritus, and that the rest originated from other

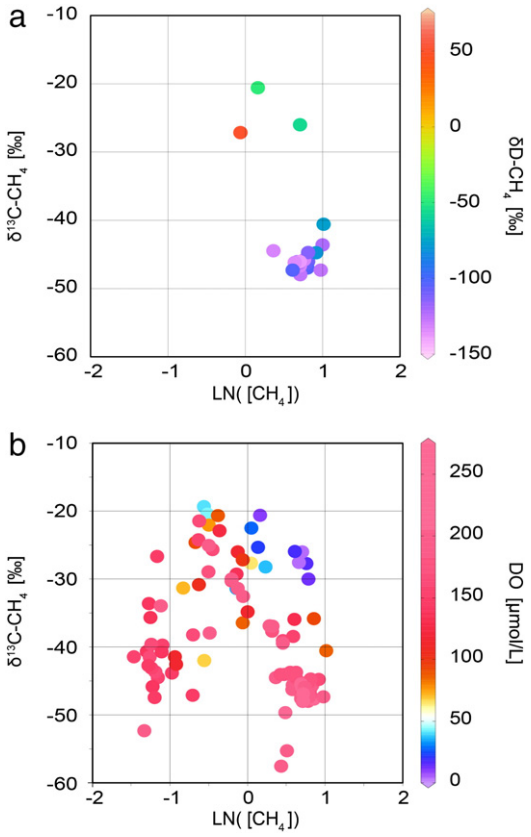


**Fig. 6.** Relationships between $\delta^{13}$C-$CH_4$ values and the natural logarithm of the dissolved $CH_4$ concentration with color coding according to the δD-$CH_4$ value (a) and dissolved oxygen concentration (b).

areas, in the cases of $\alpha = 1.013$ and 1.025, respectively. These waters have low oxygen concentrations (less than 100 μmol $kg^{-1}$; Fig. 6b), which is a feature of the ESSW from the eastern upwelling region off Peru (De Pol-Holz et al., 2009). Therefore, we conclude that the $CH_4$ in the water between 200 and 1000 m depths in the HUMB and eastern side of the E-SPSG originated mainly from the ESSW. The $CH_4$ in the ESSW possibly originates from $CH_4$ hydrate dissolution and subsequent oxidation.

The deeper data below the depth of 1500 m, except the data for the presumed hydrothermal source at station 209, plot below the estimated oxidation lines (Fig. 5). These waters have low $CH_4$ concentrations of less than 0.6 nmol $kg^{-1}$. The oxidation of $CH_4$ originating from surface primary production and subsequent degradation is almost completed below 1500 m depth. The results suggest the possibility of much smaller fractionation factors than we used here ($\alpha = 1.013$ and 1.025) and a supply of isotopically depleted $CH_4$ from seafloor sediments.

## 4. Summary

We analyzed atmospheric and dissolved $\delta^{13}$C-$CH_4$ values and $CH_4$ concentrations at 13 sites along 17°S in the subtropical South Pacific, during the R/V Mirai cruise in April–June 2009 to revisit the WOCE P21 survey line. We also analyzed dissolved δD-$CH_4$ values at three sites.

The sea–air $CH_4$ flux is high at +1.3–+4.8 μmol $m^{-2}$ $day^{-1}$ in the eastern region and the western coastal region, but it is low at −0.–0.8 μmol $m^{-2}$ $day^{-1}$ in the C-SPSG. The high fluxes at the coastal sites reflect the dominating effects of high concentrations of dissolved $CH_4$ and high wind speeds. Station 66 in the upwelling-induced anoxia region is a site of $CH_4$ accumulation (2.4 μmol $kg^{-1}$) and significant atmospheric input (+4.8 μmol $m^{-2}$ $day^{-1}$) of isotopically heavy $CH_4$ ($\delta^{13}C = -45.7$‰).

In the euphotic layer, $CH_4$ shows high concentrations (up to 2.7 nmol $kg^{-1}$) and isotopically enriched values relative to the atmospheric value of −47‰ and is supersaturated above a depth of 100 m (up to 46.9%), except for the regions in the C-SPSG. The $CH_4$ and chlorophyll *a* concentrations at the surface generally decrease from east to west and increase at the western coastal sites. This consistency suggested that active $CH_4$ productions related to the primary production cause surface $CH_4$ accumulation.

In the deeper layer, $CH_4$ shows a decrease in concentration from the surface values of about 2 nmol $kg^{-1}$ to values of less than 1 nmol $kg^{-1}$ below the depth of 1000 m, an increase in $\delta^{13}$C-$CH_4$ values from surface values near the atmospheric value of −47‰ to values exceeding −35‰ at about 1000 m, and an increase in δD-$CH_4$ values from surface values of about −130‰ to values exceeding −50‰ at about 400 m. The $^{13}$C-enriched $CH_4$ of low concentration reflects microbial oxidation of $CH_4$ with isotopic fractionation during vertical transport via particle sinking and/or zooplankton migration. The maximum values of $\delta^{13}$C-$CH_4$ exceed −30.0‰ in the water between 200 and 1000 m in the HUMB and at the east side of the E-SPSG. The relationship among the $\delta^{13}$C-$CH_4$, ln[$CH_4$], and the oxygen concentration values indicates that the $^{13}$C-enriched $CH_4$ in the HUMB and eastern side of the E-SPSG originates not only from in situ $CH_4$ production and oxidation but also from the $CH_4$ transported from the eastern upwelling region off Peru, which possibly originates from $CH_4$ hydrate dissolution and subsequent oxidation. At station 209 near the Central Lau Spreading Centers in the Lau Basin, $\delta^{13}$C-$CH_4$ values are −21.4‰ at 1000 m and −26.6‰ at 2000 m, which are much isotopically heavier than values of surrounding sites. Considering that a hydrothermal plume containing high concentrations of $CH_4$ has been reported within several kilometers of station 209 (Kim et al., 2009), we speculate that the deeply detected $CH_4$ at station 209 possibly originates from $CH_4$ hydrothermal venting that occurs somewhere near station 209.

In this study, isotopically depleted $\delta^{13}$C-$CH_4$ values (min: −57.5‰) and relatively low $CH_4$ and high chlorophyll *a* concentrations were observed in the surface water of the C-SPSG. The observed $^{13}$C-depleted $CH_4$ values may be affected by $CH_4$ emission from zooplankton guts (Sasakawa et al., 2008). Moreover, the $CH_4$ may also be affected by aerobic $CH_4$ production in phosphate-stressed water, such as the surface water in the C-SPSG (Karl et al., 2008). Observations of $CH_4$ oxidative activity, anaerobic/aerobic $CH_4$ production, and $\delta^{13}$C values of $CH_4$ originating from aerobic $CH_4$ production would contribute to more precise understanding of the surface $CH_4$ production processes.

## Acknowledgments

We thank the scientists, students and crews of the R/V Mirai, JAMSTEC, for seawater samplig and providing the hydrographic and nutrient data. This work was supported by a Grant-in-Aid for the Global COE program “From the Earth to Earths” and by the Japan Society for the Promotion of Science (JSPS) KAKENHI Grants 24740365 and 23224013. Several figures were produced using the Ocean Data View software.

## References

Botz, R., Wehner, H., Schmitt, M., Worthington, T.J., Schmidt, M., Stoffers, P., 2002. Thermogenic hydrocarbons from the offshore Calypso hydrothermal field, Bay of Plenty, New Zealand. Chem. Geol. 186, 235–248.

Coleman, D.D., Risatti, J.B., Schoell, M., 1981. Fractionation of carbon and hydrogen isotopes by methane-oxidizing bacteria. Geochim. Cosmochim. Acta 45, 1033–1037.

Conrad, R., Seiler, W., 1988. Methane and hydrogen in seawater (Atlantic Ocean). Deep-Sea Res. A 35, 1903–1917.

Damm, E., Helmke, E., Thoms, S., Schauer, U., Nöthig, E., Bakker, K., Kiene, R.P., 2010. Methane production in aerobic oligotrophic surface water in the central Arctic Ocean. Biogeosciences 7, 1099–1108. http://dx.doi.org/10.5194/bg-7-1099-2010.

De Pol-Holz, R., Robinson, R.S., Hebbeln, D., Sigman, D.M., Ulloa, O., 2009. Controls on sedimentary nitrogen isotopes along the Chile margin. Deep-Sea Res. II 56, 1042–1054.

Faure, K., Greinert, J., von Deimling, J.S., McGinnis, D.F., Kipfer, R., Linke, P., 2010. Methane seepage along the Hikurangi margin of New Zealand: geochemical and physical data from the water column, sea surface and atmosphere. Mar. Geol. 272, 170–188.
Grant, N.J., Whiticar, M.J., 2002. Stable carbon isotopic evidence for methane oxidation in plumes above Hydrate Ridge, Cascadia Oregon margin. Glob. Biogeochem. Cycles 16. http://dx.doi.org/10.1029/2001GB001851.
Holmes, M.E., Sansone, F.J., Rust, T.M., Popp, B.N., 2000. Methane production, consumption, and air–sea exchange in the open ocean: an evaluation based on carbon isotopic ratios. Glob. Biogeochem. Cycles 14, 1–10.
Houweling, S., Dentener, F., Lelieveld, J., Walter, B., Dlugokencky, E., 2000. The modeling of tropospheric methane: how well can point measurements be reproduced by a global model? J. Geophys. Res. 105, 8981–9002.
Intergovernmental Panel on Climate Change (IPCC), 2007. Climate change 2007: the physical science basis: working group I contribution to the fourth assessment. In: Solomon, S., et al. (Eds.), Report of the IPCC. Cambridge Univ. Press, New York.
Karl, D.M., Tilbrook, B.D., 1994. Production and transport of methane in oceanic particulate organic matter. Nature 368, 732–734.
Karl, D., Beversdorf, L., Björkman, K., Church, M., Martinez, A., Delong, E., 2008. Aerobic production of methane in the sea. Nat. Geosci. 1, 473–478.
Kastner, M., Kvenvolden, K.A., Lorenson, T.D., 1998. Chemistry, isotopic composition, and origin of a methane–hydrogen sulfide hydrate at the Cascadia subduction zone. Earth Planet. Sci. Lett. 156, 173–183.
Kim, J., Son, S.K., Son, J.W., Kim, K.H., Shim, W.J., Kim, C.H., Lee, K.Y., 2009. Venting sites along the Fonualei and Northeast Lau Spreading Centers and evidence of hydrothermal activity at an off-axis caldera in the northeastern Lau Basin. Geochem. J. 43, 1–13.
Kvenvolden, K.A., 1993. Gas hydrates—geological perspective and global change. Rev. Geophys. 31, 173–187.
Longhurst, A.R., 2006. Ecological Geography of the Sea. Academic Press, San Diego,.
Martinez, F., Taylor, B., Baker, E.T., Resing, J.A., Walker, S.L., 2006. Opposing trends in crustal thickness and spreading rate along the back-arc Eastern Lau Spreading Center: implications for controls on ridge morphology, faulting, and hydrothermal activity. Earth Planet. Sci. Lett. 245, 655–672.
Metcalf, W.W., Griffin, B.M., Cicchillo, R.M., Gao, J., Janga, S.C., Cooke, H.A., Circello, B.T., Evans, B.S., Martens-Habbena, W., Stahl, D.A., van der Donk, W.A., 2012. Synthesis of methylphosphonic acid by marine microbes: a source for methane in the aerobic ocean. Science 337. http://dx.doi.org/10.1126/science.1219875.
Mottl, M.J., Seewald, J.S., Wheat, C.G., Tivey, M.K., Michael, P.J., Proskurowski, G., McCollom, T.M., Reeves, E., Sharkey, J., You, C.F., 2011. Chemistry of hot springs along the Eastern Lau Spreading Center. Geochim. Cosmochim. Acta 75, 1013–1038.
Pack, M.A., Heintz, M.B., Reeburgh, W.S., Trumbore, S.E., Valentine, D.L., Xu, X., Druffel, E.R.M., 2011. A method for measuring methane oxidation rates using low levels of $^{14}$C-labeled methane and accelerator mass spectrometry. Limnol. Oceanogr. Methods 9, 245–260.
Pecher, I.A., Kukowski, N., Huebscher, C., Greinert, J., Bialas, J., the GEOPECO Working Group, 2001. The link between bottom-simulating reflections and methane flux into the gas hydrate stability zone — new evidence from Lima Basin, Peru margin. Earth Planet. Sci. Lett. 185, 343–354.
Reeburgh, W.S., 2007. Oceanic methane biogeochemistry. Chem. Rev. 107, 486–513.
Rehder, G., Collier, R.W., Heeschen, K., Kosro, P.M., Barth, J., Suess, E., 2002. Enhanced marine $CH_4$ emissions to the atmosphere off Oregon caused by coastal upwelling. Global Biogeochem. Cycles 16. http://dx.doi.org/10.1029/2000GB001391.
Sansone, F.J., Popp, B.N., Gasc, A., Graham, A.W., Rust, T.M., 2001. Highly elevated methane in the eastern tropical North Pacific and associated isotopically enriched fluxes to the atmosphere. Geophys. Res. Lett. 28, 4567–4570.
Sasakawa, M., Tsunogai, U., Kameyama, S., Nakagawa, F., Nojiri, Y., Tsuda, A., 2008. Carbon isotopic characterization for the origin of excess methane in subsurface seawater. J. Geophys. Res. 113. http://dx.doi.org/10.1029/2007JC004217.
Scranton, M.I., Brewer, P.G., 1977. Occurrence of methane in the near-surface waters of the western subtropic North Atlantic. Deep-Sea Res. 24, 127–138.
Tilbrook, B.D., Karl, D.M., 1995. Methane sources, distributions and sinks from California coastal waters to the oligotrophic North Pacific gyre. Mar. Chem. 49, 51–64.
Tsunogai, U., Ishibashi, J., Wakita, H., Gamo, T., 1998. Methane-rich plumes in Suruga Trough (Japan) and their carbon isotopic characterization. Earth Planet. Sci. Lett. 160, 97–105.
Tsunogai, U., Yoshida, N., Ishibashi, J., Gamo, T., 2000. Carbon isotopic distribution of methane in deep-sea hydrothermal plume, Myojin Knoll caldera, Izu–Bonin arc: implications for microbial methane oxidation in the oceans and applications to heat flux estimation. Geochim. Cosmochim. Acta 64, 2439–2452.
Valentine, D.L., 2011. Emerging topics in marine methane biogeochemistry. Annu. Rev. Mar. Sci. 3, 147–171.
Valentine, D.L., Blanton, D.C., Reeburgh, W.S., Kastner, M., 2001. Water column methane oxidation adjacent to an area of active hydrate dissociation, Eel River Basin. Geochim. Cosmochim. Acta 65, 2633–2640.
Wanninkhof, R., 1992. Relationship between wind speed and gas exchange over the ocean. J. Geophys. Res. 97, 7373–7382.
Whiticar, M.J., 1999. Carbon and hydrogen isotope systematics of bacterial formation and oxidation of methane. Chem. Geol. 161, 291–314.
Wiesenburg, D.A., Guinasso Jr., N.L., 1979. Equilibrium solubilities of methane, carbon monoxide, and hydrogen in water and sea water. J. Chem. Eng. Data 24, 356–360.
Wuebbles, D.J., Hayhoe, K., 2002. Atmospheric methane and global change. Earth Sci. Rev. 57, 177–210.
Yamada, K., Ozaki, Y., Nakagawa, F., Tanaka, M., Yoshida, N., 2003. An improved method for measurement of the hydrogen isotope ratio of atmospheric methane and its application to a Japanese urban atmosphere. Atmos. Environ. 37, 1975–1982.